

NONSTATIONARY MULTIPLE-ANTENNA INTERFERENCE CANCELLATION FOR UNSYNCHRONIZED OFDM SYSTEMS WITH DISTRIBUTED TRAINING

*Alexandr M. Kuzminskiy**

Bell Laboratories, Alcatel-Lucent
The Quadrant, Swindon SN5 7DJ, UK
E-mail: ak9@alcatel-lucent.com

Yuri I. Abramovich

Defence Science and Technology Organization
PO Box 1500, Edinburgh SA 5111, Australia
E-mail: Yuri.Abramovich@dsto.defence.gov.au

ABSTRACT

Adaptive interference cancellation is addressed in an orthogonal frequency division multiplexing (OFDM) system with a frame containing a number of temporally distributed pilot symbols, e.g., as in the IEEE 802.16-2004 standard. A nonstationary symbol-by-symbol switching technique based on banks of training-based and semi-blind estimators is analyzed by means of comparison with the conventional stationary pilot-based solution and with the nonasymptotic maximum likelihood benchmark especially developed for assessment of the proposed nonstationary interference cancellation algorithms.

Index Terms— Semi-blind second-order filtering, symbol-by-symbol switching, maximum likelihood benchmark, WiMAX.

1. INTRODUCTION

Multiple-antenna interference cancellation (IC) at the receiver has been the subject of a great deal of research in different application areas including wireless communications, e.g., [1] and many other articles. In wireless communications, unsynchronized transmissions in neighboring cells lead to a nonstationary asynchronous co-channel interference (CCI) scenario, where some of the interference components may not overlap with the training data of the desired signal [2], [3]. One example of such a scenario is interference mitigation on the uplink of a cellular WiMAX-compliant system based on the IEEE 802.16-2004 [4] standard addressed in [5].

A second-order statistics adaptive semi-blind (SB) algorithm for asynchronous CCI cancellation is proposed and studied in [3]. It is based on regularization of the conventional training-based least squares (LS) solution by means of the weighted covariance matrix estimated over the data interval. It is pointed out in [2] that temporally spreading the training symbols over the data slot (distributed training) could significantly simplify cancellation of the asynchronous CCI because it increases probability of overlapping between CCI and the training data. A nonstationary IC solution is presented in [5] in the case of flat fading for the CCI, where the interference statistic can be estimated on-line using averaging over the tracking subcarriers of an OFDM system.

In this paper, nonstationary semi-blind IC is studied in a distributed training scenario that is relevant for unsynchronized

WiMAX-based cellular and backhaul networks. The proposed algorithm exploits channel correlation between adjacent subcarriers and applies OFDM symbol-by-symbol (subcarrier group by subcarrier group) switching over the current OFDM symbol and the surrounding pilot symbols. Finite alphabet (FA) based switching is applied over a bank of the SB algorithms defined for each possible scenario. A nonasymptotic maximum likelihood (ML) benchmark is developed for such a solution and used for its performance assessment in the narrowband scenario for a group of subcarriers. In [6], an OFDM version of the nonstationary algorithm is studied in typical propagation conditions demonstrating significant performance improvement compared to the conventional stationary LS algorithm.

2. PROBLEM FORMULATION

We consider an uplink of an unsynchronized cellular wireless network illustrated in Fig. 1 [5]. Shaded cells in Fig. 1 represent the first ring of interference for reception of user U_0 by base station BS_0 . Users in the interfering cells transmit signals (CCI for reception of the signal of interest) to their base stations $BS_1 - BS_3$. All the users transmit similar data frames according to the IEEE 802.16-2004 standard [4] that consists of L bursts of N_{symb} OFDM symbols including preamble, which contains a training sequence for synchronization and channel estimation, data, and pilot subcarriers. All the signals in Fig. 1 propagate through similar multipath channels and are received at base station BS_0 . Only one transmission per cell is allowed.

Each frame of the desired signal may be affected by six CCI components in a three interfering cell network as illustrated in Fig. 2. A number of the training intervals in a frame of the desired signal creates a special form of a distributed training scenario. This is a nonstationary scenario because of the random switching times between different interference components even if the propagation channels are stationary over the whole data frame.

It is clear that the nonstationary interference scenario in Fig. 2 requires nonstationary interference cancellation at the receiver. Indeed, conventional stationary training-based processing (one weight vector estimated over all the preambles being used for data recovery over all the bursts) cannot be effective in this scenario because all 4 preambles in this example contain 6 interference components, but only 3 of them are presented at any time instant during the desired signal data frame.

The signal received by an antenna array of K elements can be

*Part of this work has been done in the context of the IST FP6 MEMBRANE project.

expressed as follows:

$$\mathbf{X}(n) = \mathbf{h}\mathbf{s}(n) + \sum_{m=1}^M \mathbf{g}_m \mathbf{u}_m(n) + \mathbf{Z}(n), \quad (1)$$

where $\mathbf{X}(n) = [\mathbf{x}_1(n), \dots, \mathbf{x}_{N_{\text{gr}}}(n)]$ is the $K \times N_{\text{gr}}$ matrix of the received signals for a group of N_{gr} subcarriers of the n th symbol, $\mathbf{x}_p(n)$ is the $K \times 1$ vector of the received signals for the p th subcarrier, $\mathbf{s}(n) = [s_1(n), \dots, s_{N_{\text{gr}}}(n)]$ is the $1 \times N_{\text{gr}}$ vector of the desired signals, $\mathbb{E}\{\mathbf{s}^*(n)\mathbf{s}(n)\} = \mathbf{I}_{N_{\text{gr}}}$, $\mathbb{E}\{\mathbf{s}^*(q)\mathbf{s}(g)\} = 0$, $q \neq g$, $\mathbf{u}_m(n) = [u_{m1}(n), \dots, u_{mN_{\text{gr}}}(n)]$ are the $1 \times N_{\text{gr}}$ vectors of the $m = 1, \dots, M$ independent CCI components,

$$\mathbb{E}\{\mathbf{u}_m^*(q)\mathbf{u}_m(g)\} = \begin{cases} p_m \mathbf{I}_{N_{\text{gr}}} & \text{for } q = g \in \mathcal{N}_m \\ 0 & \text{for all other } q \text{ and } g \end{cases}, \quad (2)$$

\mathcal{N}_m is the appearance interval for the m th CCI component, \mathbf{h} and \mathbf{g}_m are the $K \times 1$ complex vectors modeling linear propagation channels for the desired signal and interference, $\mathbf{Z}(n)$ is the $K \times N_{\text{scriptstylegr}}$ matrix of AWGN with variance p_0 , $\mathbb{E}\{\cdot\}$, $(\cdot)^*$, and \mathbf{I}_J respectively denote expectation, complex conjugation and the $J \times J$ identity matrix. All propagation channels are assumed to be stationary over the whole data frame and independent for different antenna elements and frames. According to [4], a data frame consists of L slots of N_{sym} symbols and the training symbol $\mathbf{s}_t = [s_{t1}, \dots, s_{tN_{\text{gr}}}]$ is located in the beginning of each slot.

We assume that reception is perfectly synchronized with the desired signal, the interference appearance intervals \mathcal{N}_m , are not known at the receiver, sufficient second-order statistics can be estimated on a symbol-by-symbol basis, i.e., $N_{\text{gr}} > K$, and the number of antenna elements exceeds the total number of signals at any time instant, i.e., $K > M/2 + 1$.

A signal estimate can be found as the output of a nonstationary spatial filter

$$\hat{\mathbf{s}}(n) = \mathbf{w}^*(n)\mathbf{X}(n), \quad (3)$$

where $\mathbf{w}(n)$ is a $K \times 1$ weight vector for the n th symbol.

The optimal weight vector can be defined as follows:

$$\mathbf{w}_{\text{opt}}(n) = \mathbf{R}^{-1}(n)\mathbf{h}, \quad (4)$$

where $\mathbf{R}(n) = \mathbb{E}\{\mathbf{X}(n)\mathbf{X}^*(n)\}$ is the covariance matrix of the received signal for the n th symbol.

A basic problem is to estimate $\mathbf{w}_{\text{opt}}(n)$ using the known training sequence and all the available training T_i and stationary data intervals D_i . Taking into account that the interference appearance intervals \mathcal{N}_m and, hence, the stationary data intervals D_i are not known at the receiver, in this paper we address a simplified problem of estimating $\mathbf{w}_{\text{opt}}(n)$ using symbol-based second-order statistics. Potentially, detection of stationary intervals can be used to improve performance. This problem is addressed in [7].

Thus, the problem is to estimate $\mathbf{w}_{\text{opt}}(n)$ using the known training sequence and symbol-based second-order statistics and compare performance to the conventional stationary training-based LS solution as well as to the nonasymptotic ML benchmark under Gaussian assumption for all variables.

3. NONSTATIONARY SOLUTION

The main idea of a symbol-by-symbol (subcarriers group by subcarrier group) switching (SSS) algorithm is to recover each symbol by means of a number of algorithms corresponding to different possible CCI scenarios with consecutive selection of the best estimates using some higher-order statistic criterion, e.g., distance from the FA. The SSS solution can be summarized as follows:

$$\hat{\mathbf{s}}(n) = \hat{\mathbf{s}}_{g_0}, \quad \hat{\mathbf{s}}_g(n) = \hat{\mathbf{w}}_g^*(n)\mathbf{X}(n), \quad (5)$$

$$g_0 = \arg \min_{g=1, \dots, G} \text{dist}_{\text{FA}}\{\hat{\mathbf{s}}_g(n)\}, \quad (6)$$

$$\text{dist}_{\text{FA}}\{\hat{\mathbf{s}}_g(n)\} = \sum_{e=1}^{N_{\text{gr}}} \min_{e=1, \dots, E} (|a_e - \hat{s}_{gq}(n)|), \quad (7)$$

where $\hat{\mathbf{s}}_g(n)$ is the g th signal candidate, G is the total number of algorithms, and a_e is the e th symbol of the FA of E symbols.

In the considered environment, the main problem is to find a set of algorithms for estimating the signal candidates $\hat{\mathbf{s}}_g(n)$. To do so, we need to analyze all the possible scenarios that can be met on a symbol-by-symbol basis. Let us consider the 3 interfering cell scenario shown in Fig. 1 and define all the possible interference scenarios for a data symbol and the left and right surrounding training symbols¹. All 6 different scenarios are presented in Fig. 3. These scenarios are different because all other possible scenarios can be transformed to the ones shown in Fig. 3 by means of renumbering the interference components and exchanging the training intervals.

Scenarios 1 - 4 are similar because all of them contain the training symbol(s) with the same set of the CCI components as the data symbol. Thus, a natural choice for these Scenarios could be the LS algorithm based on the corresponding training interval(s).

In Scenario 5, the simplest solution could be a regularized LS (RLS) algorithm [3] based on one of the training intervals, e.g.:

$$\hat{\mathbf{w}}_{\text{RLS-right}} = \left[(1 - \delta)\hat{\mathbf{R}}_{\text{t-right}} + \delta\hat{\mathbf{R}} \right]^{-1} \hat{\mathbf{r}}_{\text{t-right}}, \quad (8)$$

where $0 < \delta < 1$ is the regularization coefficient that controls the cancellation ability of the interference component that is not present in the right training interval (CCI 3 in Fig. 3), and performance degradation because of distortion of the LS solution required for cancellation of CCI 2 and 5. Efficiency of the regularized algorithm and selection of the regularization coefficient is studied in [3] in the general asynchronous CCI scenario.

The regularized algorithm (8) can be applied in the general case with a number of interference components in the data interval that are not present in the training interval. In the particular Scenario 5, where only one new CCI component appears in the data interval, specific semi-blind algorithm with "cleaning" of the training intervals can be exploited as proposed in [6]. We will refer to this estimator as the semi-blind (SB) solution.

Scenario 6 is similar to Scenario 5. The difference is that one of the training symbols (the left one in Fig. 3) is affected by two CCI components not present on the other intervals. This means that the regularized solution (8) and its natural "cleaned" modification, i.e., the regularized SB (RSB) algorithm, can be applied in this case.

¹For simplicity, the data symbols in the last slot are not considered; they can be addressed similarly.

Now, we have the algorithms to apply in all the situations that may appear in the general scenario shown in Fig. 2. Taking into account that Scenarios 2-4, and 6 are asymmetrical in terms of the left/right training intervals, we need to include both left and right versions of the corresponding estimators to the algorithm banks to be used by the SSS algorithm (9) - (15). The first bank can be formed from the semi-blind algorithms as follows:

Bank 1: 1) $\mathbf{w}_{\text{LS-left+right}}$; 2) $\mathbf{w}_{\text{LS-left}}$; 3) $\mathbf{w}_{\text{LS-right}}$; 4) \mathbf{w}_{SB} ; 5) $\mathbf{w}_{\text{RSB-left}}$; 6) $\mathbf{w}_{\text{RSB-right}}$.

The SSS algorithm based on Bank 1 will be referred to as the semi-blind SSS estimator (SBSSS).

A simplified bank of algorithms can be formed from only the regularized solutions as follows:

Bank 2: 1) $\mathbf{w}_{\text{RLS-left+right}}$; 2) $\mathbf{w}_{\text{RLS-left}}$; 3) $\mathbf{w}_{\text{RLS-right}}$.

The SSS algorithm based on Bank 2 will be referred to as the regularized SSS estimator (RSSS).

4. NONASYMPTOTIC ML BENCHMARK

For the Gaussian assumption for all variables, we can define the ML solution for each scenario shown in Fig. 3 similarly to [3], taking into account the particular sets of the CCI components for the data and the left and right training symbols:

$$\hat{\mathbf{s}}_{\text{ML}} = \hat{\mathbf{w}}_{\text{ML}}^* \mathbf{X}, \quad (9)$$

$$\hat{\mathbf{w}}_{\text{ML}} = \hat{\mathbf{A}}_{\text{ML}}^{-1} \hat{\mathbf{c}}_{\text{ML}}, \quad (10)$$

$$\left[\hat{\mathbf{A}}, \hat{\mathbf{A}}_{\text{t-left}}, \hat{\mathbf{A}}_{\text{t-right}} \right]_{\text{ML}} = \arg \max_{\mathbf{c}, \mathbf{c}_q, p_q, d} \gamma \gamma_{\text{t-left}} \gamma_{\text{t-right}}, \quad (11)$$

$$\gamma = \frac{\exp(K) \det(\mathbf{A}^{-1} \hat{\mathbf{R}})}{\exp[\text{tr}(\mathbf{A}^{-1} \hat{\mathbf{R}})]}, \quad (12)$$

$$\gamma_{\text{t}} = \frac{\exp(K+1) \det(\bar{\mathbf{A}}_{\text{t}}^{-1} \hat{\mathbf{R}}_{\text{t}})}{\exp[\text{tr}(\bar{\mathbf{A}}_{\text{t}}^{-1} \hat{\mathbf{R}}_{\text{t}})]}, \quad (13)$$

$$\mathbf{A} = \mathbf{c} \mathbf{c}^* + \sum_{q \in Q} p_q \mathbf{c}_q \mathbf{c}_q^* + d \mathbf{I}_K, \quad (14)$$

$$\bar{\mathbf{A}}_{\text{t}} = \begin{bmatrix} 1 & \mathbf{c}^* \\ \mathbf{c} & \mathbf{c} \mathbf{c}^* + \sum_{q \in Q_{\text{t}}} p_q \mathbf{c}_q \mathbf{c}_q^* + d \mathbf{I}_K \end{bmatrix} > 0, \quad (15)$$

where γ and γ_{t} are the likelihood ratios defined for the data and training symbols (left and right), $\hat{\mathbf{R}}$ and $\hat{\mathbf{R}}_{\text{t}} = \begin{bmatrix} \hat{p}_{\text{t}} & \hat{\mathbf{r}}_{\text{t}}^* \\ \hat{\mathbf{r}}_{\text{t}} & \hat{\mathbf{R}}_{\text{t}} \end{bmatrix}$ are the sufficient statistics for the data and training symbols (left and right) and the admissible sets of optimization parameters \mathbf{A} and $\bar{\mathbf{A}}_{\text{t}}$ follow the CCI structures for the corresponding scenarios captured in the scenario specific sets of the CCI indexes summarized in Table 1.

Table 1. CCI indexes for optimization parameters in (14), (15)

Scenario	1	2	3	4	5	6
Q	1,2,3	2,3,4	2,4,5	2,4,6	2,3,5	2,4,5
$Q_{\text{t-left}}$	1,2,3	1,3,4	1,3,5	1,3,5	1,3,5	1,3,5
$Q_{\text{t-right}}$	1,2,3	2,3,4	2,4,5	2,4,6	2,4,5	2,4,6

To evaluate the ML benchmark performance for different scenarios we need initialization of all the parameters and an optimization algorithm to solve the nonlinear constrained problem (9) - (15). Generally, identification algorithms for all the scenarios are required

for initialization. Then, an optimization outliers selection procedure can be applied similarly to [3] to estimate the ML benchmark performance for simulated or measured data. This benchmark is studied in [8] in the context of Scenario 5 shown in Fig. 3.

In this paper we accept an initialization from the actual parameters suitable only for simulated data. This initialization allows us to take into account finite amount of data effects and significantly simplify the problem, but it may lead to an optimistic performance compared to realistic initialization.

5. SIMULATION RESULTS

We simulated a five-element antenna array ($K = 5$) and the CCI scenarios illustrated in Fig. 2 and 3. The desired signal and interference are generated as independent streams of random symbols $(\pm 1 + \pm j)/\sqrt{2}$. All propagation channels are simulated as independent complex Gaussian vectors with unit variance and zero mean. Signal-to-interference ratio SIR=0 dB is assumed in all narrowband simulations. Bit error rate (BER) performance is estimated over 10^4 trials with independent channel and data realizations. The routine "fmincon" from the MATLAB Optimization Toolbox is used for maximization in (9) - (15). The minimum mean square error (MMSE) for the known parameters is used as the asymptotic benchmark.

Fig. 4 shows the typical results for the different scenarios in Fig. 3 for $N_{\text{gr}} = 16$ and $\delta = 0.2$. The legend in the first plot (Scenario 1) indicates the algorithms applied in all the scenarios. The legends in other plots indicate the best algorithms in the particular scenarios included in Bank 1. The following observation can be made from Fig. 4: the results in Scenario 1 illustrate the LS algorithm that exploits all the available training data is very close to the ML solution in this case; in all other scenarios, LS estimated over both training intervals demonstrates very poor performance compared to the benchmarks and the semi-blind algorithms; in Scenario 3 (similar results are observed in Scenarios 2 and 4), the best results are obtained by means of LS based on the training interval with the same set of the CCI components as for the data interval. Its performance degradation is less than 0.5 dB at 1% BER compared to the ML benchmark; in Scenario 5, the SB demonstrates the best results that are about 1 dB worse compared to the ML benchmark at 1% BER, RLS shows further 2 dB degradation, but it is still much better compared to LS at same BER level; Scenario 6 is the most difficult one. The best results in this case are obtained with RSB and they are 5 dB worse than the ML benchmark and RLS shows further 1.5 dB of performance degradation at 1% BER.

The BER performance in the 3-cell case shown in Fig. 2 is given in Fig. 5. Additional to the algorithms and benchmarks, one more curve (SBSSS-known) is plotted in Fig. 5, which represents the algorithms from Bank 1 with on-line selection of the known symbol-based scenario instead of the practical FA-based selection as in (6), (7). In this case, the same information is used for the ML benchmark and SBSSS-known estimates. So, for fair comparison we should consider the benchmark and SBSSS-known rather than SBSSS results, but one can see that for a wide range of N_{gr} , SBSSS only slightly outperforms SBSSS-known because of some opportunistic gain (on-line comparison of a number of random realizations instead of selection of the best average performance).

To summarize, the simulation results show that all the nonstationary switching algorithms considered here significantly outper-

form the conventional LS solution; in the general scenario, the SBSSS algorithm demonstrates the best results that are from 0.5 dB to 2 dB worse compared to the ML benchmark depending on the available amount of data; the simplified RSSS algorithm is very close to SBSSS for $N_{gr} = [16, 24]$, but it demonstrate significant performance degradation for $N_{gr} = 8$.

6. CONCLUSION

The adaptive nonstationary interference cancellation technique has been proposed for an asynchronous OFDM system with a frame containing a number of temporally distributed pilot symbols. The symbol-by-symbol benchmark has been proposed and applied for assessment of the final amount of data effects. It has been demonstrated that the proposed nonstationary solutions significantly outperform the conventional stationary training-based estimator and demonstrate performance that is reasonably close to the benchmark in typical scenarios.

7. REFERENCES

- [1] D. Astely, B. Ottersten, "Spatio-temporal interference rejection combining," in Smart Antennas - State of the Art, T. Kaiser, et al, Eds., Hindawi, 2005, ch. 2.
- [2] C. Martin, B. Ottersten, "On robustness against burst unsynchronized co-channel interference in semi-blind detection," in Proc. 34th Asilomar Conf. Sig., Syst. and Comp., pp. 946-450, 2000.
- [3] A. M. Kuzminskiy, Y. I. Abramovich, "Second-order asynchronous interference cancellation: regularized semiblind technique and nonasymptotic maximum likelihood benchmark," Signal Processing, vol. 86, no. 12, pp. 3849-3863, 2006.
- [4] IEEE 802.16-REVd/D5-2004, "IEEE Standard for Local and Metropolitan Area Networks - Part 16: Air Interface for Fixed Broadband Wireless Access Systems," May 2004.
- [5] M. Nicoli, M. Sala, O. Simeone, L. Sampietro, C. Santacesaria, "Adaptive array processing for time varying interference mitigation in IEEE 802.16 systems," in Proc. PIMRC, 2006.
- [6] A. M. Kuzminskiy, Y. I. Abramovich, "Switching space-time interference cancellation for OFDM systems with unsynchronized cells," in Proc. ISCCSP, 2008.
- [7] MEMBRANE Deliverable D4.1.2, "IA/MIMO-enabled techniques and reconfigurable routing," July 2007, <http://www.ist-membrane.org>
- [8] A. M. Kuzminskiy, Y. I. Abramovich, "Semi-blind interference cancellation with distributed training," in Proc. EUSIPCO, 2007.

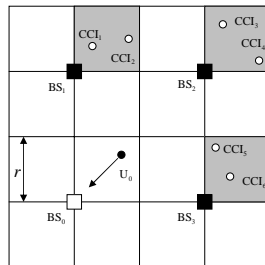


Fig. 1. Uplink layout for a wireless cellular system.

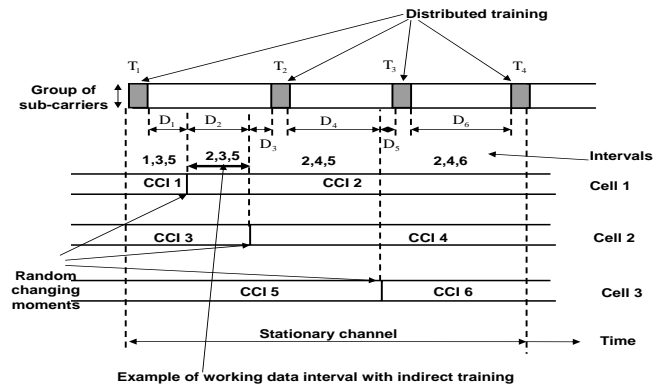


Fig. 2. Asynchronous scenario for three interfering cells.

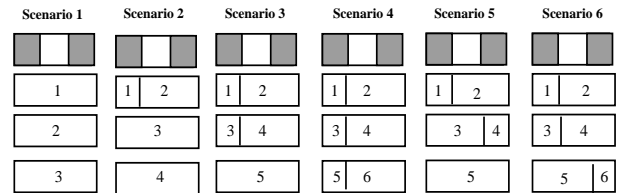


Fig. 3. Symbol-by-symbol scenarios for three interfering cells.

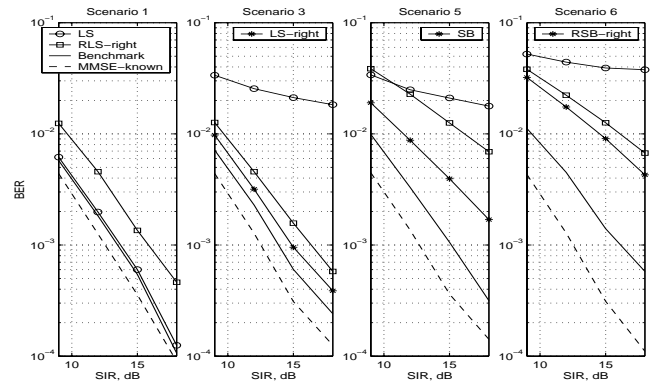


Fig. 4. Typical BER results in different scenarios in Fig. 3.

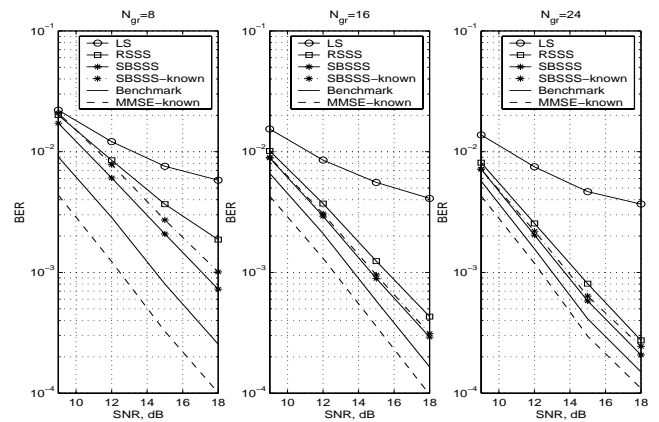


Fig. 5. BER performance in the three-cell scenario.